Trop J Nat Prod Res, July 2025; 9(7): 3162 - 3172 **ISSN 2616-0684 (Print)**
ISSN 2616-0692 (Electronic)

Tropical Journal of Natural Product Research

Available online at https://www.tjnpr.org

Original Research Article

Green Synthesis of Silver Nanoparticles from *Tribulus terrestris* and Investigation of Their Antioxidant and Anticancer Activities against MG-63 Osteosarcoma Cells

Rachel D Kirubai S[1*], Velvizhy Ramalingam[2], Subhashree Manavalan Venkatraman[3], Panneerselvam T[1], Mukesh Kumar Dharmalingam Jothinathan[4], Iadalin Ryntathiang[4], Archana Behera[4]

[1.] *Department of Microbiology, Adhiparasakthi College of Arts and Science (Autonomous), G. B. Nagar, Kalavai-632506, Affiliated to Thiruvalluvar University, Serkkadu-632115, Tamil Nadu, India.*
[2.] *Department of Pharmacology, Sri Lakshmi Narayana Institute of Medical sciences (SLIMS), Puducherry, India.*
[3.] *Department of Physiology, Saveetha Medical College and Hospital, Saveetha Institute of Medical and Technical Sciences (SIMATS), Saveetha University, Chennai, Tamil Nadu, India.*
[4.] *Department of Biochemistry, Saveetha Medical College and Hospital, Saveetha Institute of Medical and Technical Sciences (SIMATS), Saveetha University, Chennai, Tamil Nadu, India.*

ARTICLE INFO

Article history:
Received 10 February 2025
Revised 23 May 2025
Accepted 03 June 2025
Published online 01 August 2025

ABSTRACT

The increasing interest in green nanotechnology has led to the use of medicinal plants for synthesizing nanoparticles with bio-medical applications. This study focuses on synthesizing silver nanoparticles (AgNPs) using the aqueous leaf extract of *Tribulus terrestris*, aiming to evaluate their anti-oxidant, enzyme inhibitory and anti-cancer activities. The synthesis was confirmed through UV-Vis spectroscopy, where the plant extract showed a peak at 282 nm and AgNPs exhibited a surface plasmon resonance peak at 430 nm. Fourier Transform Infrared (FTIR) spectroscopy revealed functional groups of plant extract as -OH, -C=O and -NH, which were involved in the stabilization and reduction of the AgNPs. X-ray diffraction (XRD) confirmed the nanoparticles as crystal in nature, while Scanning Electron Microscopy (SEM) showed their spherical morphology. Dynamic Light Scattering (DLS) demonstrated good nanoparticle stability. Biological testing revealed significant anti-oxidant activity, with DPPH (78.27%), ABTS (76.55%) and iron chelation (79.74%) at 640 µg/mL. Enzyme inhibition assays showed high inhibition of polyphenol oxidase (91.99%) and peroxidase (98.74%). The AgNPs also exhibited promising anti-cancer potential, with a 78.34% reduction in MG-63 osteosarcoma cell viability at 80 µg/mL Gene expression analysis revealed upregulation of Caspase 9 and Bax and downregulation of Bcl-2, suggesting an apoptotic pathway in the cancer cells. In conclusion, *T. terrestris* synthesized AgNPs show great promise for use in therapeutic applications, particularly in cancer treatment.

Keywords: Green synthesis, *Tribulus terrestris*, Anti-oxidant activity, Cytotoxicity, Anti-cancer activity.

Introduction

In recent years, nano biotechnology has gained considerable significance in materials science, biology and medical applications.[1,2] The synthesis of nanoparticles plays a crucial role in nanotechnology and various methods exist for their fabrication, including phase transfer, microwave-assisted, electro-chemical, sono-chemical, reverse micelle, radiation assisted and photochemical techniques.[3] Among metal nanoparticles, silver nanoparticles (AgNPs) stand out due to their unique optical, electrical and synergistic properties, making them highly concentrated and of significant interest in various fields. As a noble metal, silver exhibits notable anti-bacterial and larvicidal properties and it has been extensively incorporated into nanoparticle synthesis through physical, chemical and biological methods.

*Corresponding author. Email: rachelanbu15@gmail.com
Tel: +91 9442661987

Citation: Rachel Deva Kirubai S, Ramalingam V, Venkatraman SM, Panneerselvam T, Jothinathan MKD, Ryntathiang I, Behera A. Green Synthesis of Silver Nanoparticles from *Tribulus terrestris* and Investigation of Their Antioxidant and Anticancer Activities against MG-63 Osteosarcoma Cells. Trop J Nat Prod Res. 2025; 9(7): 3162 – 3172 https://doi.org/10.26538/tjnpr/v9i7.29

Official Journal of Natural Product Research Group, Faculty of Pharmacy, University of Benin, Benin City, Nigeria

AgNPs are rapidly gaining attention due to their remarkable physical, chemical and biological characteristics, small size and large specific surface area.[4] AgNPs have been used in medical treatments for centuries, primarily for their anti-microbial properties.[5] Silver based compounds are well known for their ability to eliminate microbes, making them valuable for advanced bio-medical applications such as wound healing, drug delivery, tissue scaffolding and anti-microbial coatings.[6] Recently, interest in AgNPs has grown due to the rise of antibiotic resistance in various microbial pathogens. AgNPs are appreciated for their chemical, physical properties, non-toxic nature, broad spectrum of bactericidal and anti-cancer effects, in addition to their therapeutic potential. However, several traditional nanoparticle synthesis methods still involve hazardous chemicals, posing health and environmental risks.[7] AgNPs, due to their novel properties are increasingly being used in diverse applications, including medical, industrial and environmental fields. Their small size and large surface area enhance their effectiveness in these applications. In recent studies, bio-active AgNPs synthesized from various plant species, showing strong anti-oxidant and anti-microbial properties.[8] Despite the known medicinal properties of *Tribulus terrestris*, particularly in its fruits and leaves, there has been scientific investigation into the potential health benefits of these plant parts.[9] Osteosarcoma is a type of malignant bone tumor that typically develops in children, young adults and adolescents. It derives from osteoblasts, the cells responsible for generating new bone tissue. Given this context, the research progresses with the synthesis of AgNPs using *T. terrestris*, with an emphasis on their potential bio-medical applications.[10] The novelty of this study lies in its

contribution to exploring the therapeutic potential of AgNPs, offering new possibilities in medicinal applications. The study aims to synthesize AgNPs using *T. terrestris* leaf extract through a green synthesis method and evaluate their anti-oxidant, enzyme inhibitory and anti-cancer activities, particularly against MG-63 osteosarcoma cells. This research seeks to explore the potential bio-medical applications of *T. terrestris* derived AgNPs, focusing on their effectiveness in combating oxidative stress and inhibiting the proliferation of osteosarcoma cells.

Materials and Methods

Plant Collection and Preparation

Leaves of *T. terrestris* were collected from Cheyyar, Tamil Nadu, India (GPS coordinates: 12.6607° N, 79.5435° E) on 7th June 2023. The plant was identified and authenticated by botanical taxonomy specialists at the Siddha Central Research Institute, Chennai- 600106. A voucher specimen (Voucher No. T06062301T) was deposited at the institute for future reference. After harvesting, the leaves were carefully washed, air-dried and then pulverized into a fine powder. A 10g sample of the powdered leaves was then combined with 100 mL of distilled H_2O and subjected to boiling for 30 min at 70 ºC. The resultant aqueous leaf extract was filtered using Whatman filter paper No. 1 and preserved at 4 ºC for future utilization.

Green synthesis of silver nanoparticles

Initially 10 mL of the aqueous leaf extract from *T. terrestris* was introduced into a solution containing 90 mL of silver nitrate (1 mM $AgNO_3$) and the mixture was subjected to stirring for 3 h at 80 ºC. The solution indicated the synthesis of AgNPs by changing from yellow to dark brown color, as noted in a previous work.[11] The synthesized nanoparticles were subsequently centrifuged for 15 min at 10,000 rpm to acquire pellets. This treatment was conducted thrice to eradicate any remaining free silver potentially linked to the AgNPs. The final AgNPs produced through this green synthesis method were labeled as AgNPs, later freeze dried and stored at 4 ºC for further examination.[12]

Characterization of Silver Nanoparticles

The bio reduction of AgNPs was monitored using Ultraviolet-visible (UV-Vis) spectroscopy (Shimadzu UV-1800, Cole-Parmer India Pvt Ltd, Mumbai, India), which operated within the wavelength range of 200 to 800 nm. To investigate the crystalline structure, X-ray diffraction (XRD) analysis was performed using an X'PERT PRO PAN analytical system (Philips, Amsterdam, Netherlands). The surface morphology and size of the nanoparticles were evaluated using scanning electron microscopy (SEM) with a JEOL-6390LA/OXFORD XMX N (Jeol USA Inc., Peabody, MA, USA) at an accelerating voltage of 0.5 to 30 kV. The size and zeta potential of synthesized AgNPs were analyzed using the dynamic light scattering (DLS) technique (Brookhaven Cooperation, NY, USA). Additionally, Fourier transform infrared spectroscopy (FTIR) was used to analyze the functional groups present, employing a Perkin Elmer-Tensor 27 (Bruker, Billerica, MA, USA) with a wavelength range of 400 to 4000 cm^{-1}.

In vitro Anti-oxidant Activity

DPPH Assay

The DPPH radical scavenging potential was evaluated using a colorimetric assay as previously described.[13] DPPH of 0.1 mM solution was prepared in methanol and kept in the dark for 20 min to stabilize the absorbance. This solution was combined with synthesized AgNPs at concentrations ranging from 5 to 640 µg/mL in separate test tubes. The mixtures were incubated at 37°C in the dark for 30 min. After incubation, the absorbance was observed at 517 nm was recorded using a spectrophotometer (Shimadzu UV-1800, Cole-Parmer India Pvt Ltd, Mumbai, India). A decrease in absorbance indicates the radical scavenging activity of the AgNPs, with Vitamin C serving as the control standard. The IC_{50} value was determined from the average ± standard deviation (SD) based on the concentrations tested. The percentage inhibition was calculated using equation 1.

$$\% \text{ Inhibition} = \left[\frac{\text{Absorbance of control} - \text{Absorbance of sample}}{\text{Absorbance of control}}\right] \times 100$$

ABTS Assay

The ABTS radical scavenging potential of the synthesized nanoparticles was determined using a modified radical cation decolorization technique, which evaluates the electron-donating ability of test compounds.[14] To generate the $ABTS^+$ radical, equal volumes (1:1) of 7 mM ABTS and 2.45 mM potassium persulfate ($K_2S_2O_8$) solutions were mixed and incubated in the dark at 37°C for 24-48 h. The resulting $ABTS^+$ solution was diluted in a 1:25 ratio and 300 µL of synthesized AgNPs at concentrations as 5, 10, 20, 40, 80, 160, 320 and 640 µg/mL was added to 3.0 mL of the freshly diluted $ABTS^+$ solution. The mixture was thoroughly vortexed and incubated at 37°C for a 30 min. The absorbance was then recorded at λmax=745 nm using a UV-Visible spectrophotometer (Shimadzu UV-1800, Cole-Parmer India Pvt Ltd, Mumbai, India). The $ABTS^+$ radical scavenging percentage was calculated using equation 1.

Iron Chelating Ability Assay

The method for evaluating the iron (II) binding capacity of the test sample follows the approach outlined in the literature.[15] In this assay, the formation of a red complex between ferrous ions and ferrozine, which absorbs light at λmax = 562 nm was used to monitor ferrous ions. To perform the assay, 2.0 mL of solutions containing iron chelators at concentrations of 5, 10, 20, 40, 80, 160, 320 and 640 µg/mL were mixed with 0.4 mL of 2 mM $FeSO_4$ solution. After adding 0.2 mM ferrozine, the reaction mixture was incubated for 10 min at 37°C and the absorbance was measured at λmax = 562 nm. The percentage of inhibition was calculated using equation 1.

Enzyme Assays

Polyphenol Oxidase Assay

Polyphenol Oxidase (PPO) activity was measured based on the protocol with minor modifications.[16] Nanoparticles were prepared at concentrations of 160, 320 and 640 µg/mL in 3 mL of 0.1M $NaPO_4$ buffer (pH 6.5). To start the reaction, 0.2 mL of 0.01 M catechol was introduced and the absorbance variation was documented every 30 sec at λmax = 495 nm for a duration of 2 min. The enzyme activity was quantified in units per milliliter.

Peroxidase Assay

Nanoparticles at doses of 160, 320 and 640 ng/mL served as the enzyme source. A reaction mixture was created by combining 3.0 mL of buffer solution, 0.05 mL of guaiacol solution, 0.1 mL of enzyme extract and 0.03 mL of H_2O_2 solution in a cuvette.[17] The absorbance was recorded at λmax = 470 nm. The oxidase activity of the nanoparticles was determined using the equation 2:

$$\text{Activity } (\text{U.mL} - 1) = \left[\frac{(\text{AFsample} - \text{AIsample}) - (\text{AFblank} - \text{AIblank})}{(0.001 \times \text{t})}\right]$$

Cell Culture Studies

Cell Line Maintenance

The MG-63 human osteosarcoma cell line was procured from the National Centre for Cell Science (NCCS), Pune, India. Cells were cultured in T25 flasks containing Dulbecco's Modified Eagle Medium (DMEM) supplemented with 10% fetal bovine serum (FBS) and 1% antibiotic solution under standard conditions. They were incubated at 37 °C in a humidified environment with 5% CO_2. Once the cells reached confluence, they were detached using trypsin and then passaged for further cultivation.

In Vitro Anti-Proliferative Effect of AgNPs *on MG-63 Osteosarcoma Cell Line by MTT Assay*

The cytotoxic effect of AgNPs on MG-63 osteosarcoma cells was assessed using the MTT assay, which detects cellular metabolic activity through the reduction of yellow tetrazolium dye into insoluble purple formazan crystals by viable cells.[18] Cells were seeded into 96 well plates at a density of 5×10^3 cells per well and incubated for 24 h. Following this, the cells were washed twice with serum free medium and incubated in the same for 3 h at 37 °C. They were then treated with varying concentrations of AgNPs (1.25-40 µg/mL) for an additional 24 h. After the exposure period, the treatment medium was removed and each well received 100 µL of MTT solution (0.5 mg/mL in DMEM). After 4 h of incubation, the medium was carefully discarded and the resulting formazan crystals were dissolved in 100 µL of DMSO. Absorbance was recorded at 570 nm using a microplate reader. The percentage of viable cells was calculated relative to the untreated control using the equation 3:

$$\% \text{ Cell viability} = \left[\frac{\text{A570 nm of treated cells}}{\text{A570 nm of control cells}}\right] \times 100$$

Morphology Analysis

Following the identification of the appropriate doses (IC_{50}: 5 and 10 µg/mL) via MTT evaluation, the morphological variations of MG-63 cells were examined. The cells were treatment with AgNPs for 24 h and were subsequently rinsed with PBS (pH 7.4). Cell morphology was examined utilizing a phase contrast microscope.

Gene Expression Analysis

Gene expression analysis of Bax, Caspase 9 and Bcl-2 was performed using real-time PCR. Total RNA was extracted using the TRIzol reagent (Sigma-Aldrich), and complementary DNA (cDNA) was synthesized utilizing the PrimeScript™ First Strand cDNA Synthesis Kit (Takara Bio, Japan). Quantitative PCR amplification of target genes was performed with gene-specific primers using the GoTaq® qPCR Master Mix (Promega, USA) The PCR reactions were conducted using a CFX96 PCR machine (Bio-Rad). The comparative CT approach was employed for data analysis, with fold changes determined via the 2-ΔΔCT method (Schmittgen and Livak).

Statistical Analysis

The data were examined utilizing One-way ANOVA, succeeded by a student's t-test, employing GraphPad Prism version 7.0 software. The data were expressed as the mean ± standard deviation (SD) based on triplicate measurements. Statistical significance was set at $p < 0.05$.

Results and Discussion

UV-Vis Spectroscopic Properties of Silver Nanoparticles and Plant Extract

In the present study, the *T. terrestris* plant extract was utilized for the biosynthesis of AgNPs. The UV-Vis spectrum of the plant extract exhibited a peak at 282 nm (Fig. 1a), indicating the presence of specific bio-active compounds, which are responsible for the reduction of silver ions into nanoparticles. The characteristic absorption at this wavelength can be attributed to the presence of phenolic compounds and flavonoids in the plant extract, which are known to have strong reducing properties.

The formation of AgNPs was initially confirmed by a noticeable color change when the plant extract was added to the $AgNO_3$ solution. The initially transparent yellow solution quickly transitioned to a deep black color, indicating the successful synthesis of AgNPs. This color change is attributed to surface plasmon resonance (SPR), a characteristic optical property of nanoparticles. The UV-Vis absorption spectrum of the AgNPs exhibited a prominent absorbance peak at 410 nm, which is typical for AgNPs and supports their successful formation showed in (Fig.1b). Similar UV absorption peaks were reported for nanoparticles synthesized from *Persicaria senegalensis* (431 nm).[19] In addition, a peak around 420-430 nm is commonly observed for AgNPs synthesized from various plant sources, indicating that the nanoparticle size and shape can be influenced by the plant extract composition. Recent studies have reported the formation of AgNPs with slightly varying absorption peaks, such as those synthesized from *Pongamia pinnata* and *Cissus quadrangularis*.[20,21] This absorption range indicates the formation of spherical or quasi-spherical AgNPs, which can be confirmed through additional characterization techniques like SEM and TEM. Moreover, the UV-Vis spectra provide insight into the stability of AgNPs. A narrow, sharp peak suggests the uniform size and high monodispersity of the nanoparticles, which is crucial for their potential bio-medical applications. The SPR peak shift observed in certain studies, such as AgNPs from *Azadirachta indica*, indicates a change in particle size or agglomeration, which can be controlled by optimizing the synthesis parameters.[22]

FTIR Spectrum Analysis of Silver Nanoparticles and Plant Extract

The Fourier Transform Infrared (FTIR) spectrum of AgNPs synthesized using *T. terrestris* plant extract revealed several characteristic peaks corresponding to specific functional groups in the plant molecules (Fig. 2a and Table 1).

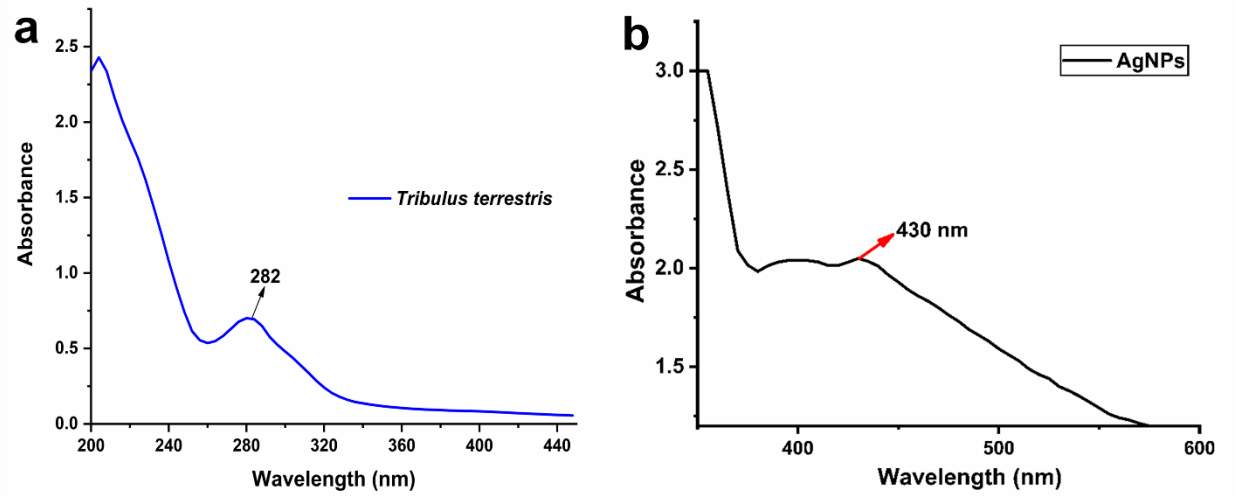

Figure 1 a): UV-Vis spectrum of plant extract, **b)** UV-Vis spectrum of silver nanoparticles

ISSN 2616-0684 (Print)
ISSN 2616-0692 (Electronic)

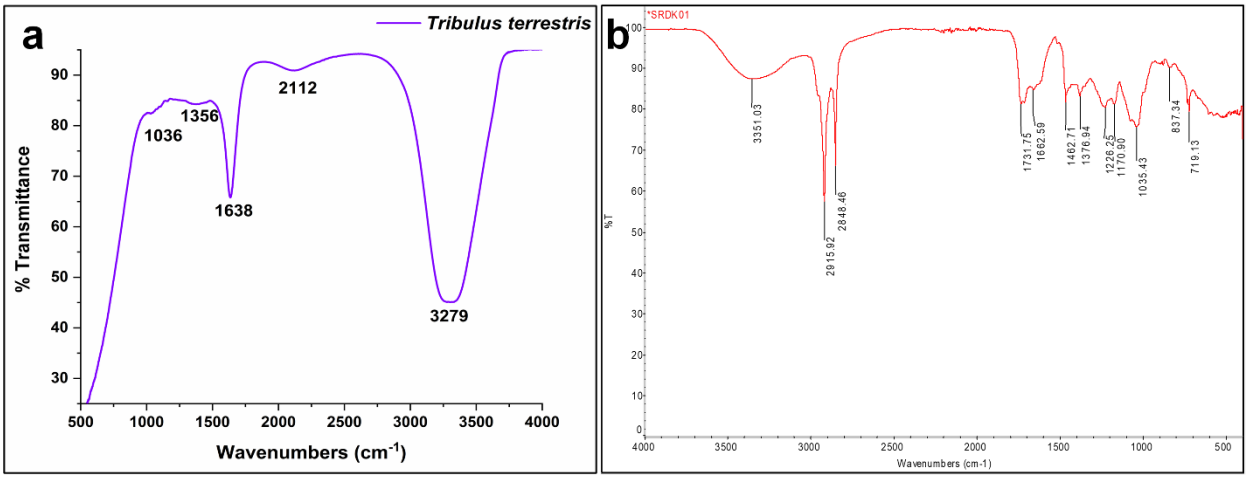

Figure 2 a): FTIR spectrum of the plant extract, **b)** FTIR spectrum of the synthesized silver nanoparticles

The peak at 1036 cm^{-1} is attributed to the C-O stretching vibration, commonly associated with phenolic groups or alcohols, suggesting the presence of hydroxyl containing compounds in the *T. terrestris* extract that may play a role in stabilizing the nanoparticles. The 1356 cm^{-1} peak corresponds to C-H bending vibrations of alkyl groups, indicating that aliphatic hydrocarbons from the plant extract are involved in the synthesis and stabilization of AgNPs. The absorption at 1638 cm^{-1} is linked to the C=O stretching vibration, characteristic of carbonyl groups, likely originating from carboxylic acids, esters or amide bonds in the *T. terrestris* compounds, which are involved in reducing and capping the AgNPs. The peak at 2112 cm^{-1} corresponds to C≡C stretching, possibly associated with alkynes or nitriles in the plant extract, contributing to the formation of the nanoparticles. Lastly, the broad band at 3279 cm^{-1} is attributed to O-H stretching, indicative of hydroxyl groups, likely derived from phenolic compounds in *T. terrestris* that aid in the reduction of silver ions and stabilization of the AgNPs.

Table 1: FTIR spectrum analysis of different functional groups present in plant extract

S. No	Wave number (cm^{-1})	Intensity	Bond responsible	Functional Groups
1	1036	Medium	C-O Stretching	Phenolic Groups or Alcohols
2	1356	Medium	C-H Bending	Alkyl Groups
3	1638	Strong	C=O stretching	Carbonyl Groups
4	2112	Medium	C≡C Stretching	Alkynes Groups
5	3279	Strong	O-H Stretching	Hydroxyl Groups

Further analysis of the synthesized AgNPs (Fig. 2b and Table 2) revealed eight distinct functional groups, shedding light on the chemical composition and possible interactions between the plant extract and the nanoparticles. Key functional groups identified include the N-H stretch of amines (3351.03 cm^{-1}), C-H stretch of alkanes (2915.92 cm^{-1}), O-H bend associated with alkynes (2848.46 cm^{-1}), C-H bend in aldehydes (1731.75 cm^{-1}) and C-H stretch of carboxylic acids (1662.59 cm^{-1}). These groups suggest that the plant extract plays a crucial role in stabilizing the AgNPs by capping and reducing silver ions during nanoparticle formation. In a similar study using *Decaschistia crotonifolia*, functional groups such as O-H stretch (3283 cm^{-1}), C-H stretch (2931 cm^{-1}) and C=C stretch (1636 cm^{-1}) were also identified.[23] For instance, FTIR analysis of AgNPs synthesized using *Spirulina maxima* showed absorption peaks at 2929 cm^{-1} (aliphatic CH stretching), 1625 cm^{-1} (carboxyl C–O stretching) and 1036 cm^{-1} (amine N–H vibrations), indicating the involvement of esters, amines, aldehydes, alkenes, alkanes and carboxylic acids in the synthesis process.[24] Similarly, a study on *Achillea wilhelmsii* leaf extract mediated AgNPs identified FTIR peaks at 2927 cm^{-1} (C–H stretching of alkanes), 1655 cm^{-1} (carbonyl groups in amide linkages) and 3446 cm^{-1} (O–H bond), suggesting the participation of alcohols, carboxylic acids, alkenes and amides in the nanoparticle formation.[25] These findings align with your study, emphasizing the diverse functional groups present in plant extracts that facilitate the reduction and stabilization of AgNPs. The presence of these functional groups not only aids in the synthesis of AgNPs but also contributes to their stability and potential biological activities. These bio-molecules act as reducing and capping agents, ensuring the formation of stable and biologically active AgNPs.

X-Ray Diffraction Analysis

In Fig. 3 confirms the crystalline form of the AgNPs through XRD analysis. The XRD pattern exhibited prominent diffraction peaks at particular 2θ values, indicating the crystalline planes of the AgNPs. Peaks at 100, 102, 002, 101 and 112 correspond to the face centered cubic (FCC) structure of silver, confirming the well-defined crystalline structure of the AgNPs. The observed peaks align with those reported in another study involving *Tagetes erecta*.[26]

Table 2: FTIR spectrum analysis of different functional groups present in silver nanoparticles

S. No	Wave number (cm^{-1})	Intensity	Bond responsible	Functional Groups
1	719.13	Medium	C-H	Alkenes
2	837.34	Strong	N-H	Amines
3	1035.43	Medium	N-H	Aliphatic Amines
4	1170.90	Medium	C–H	Alkenes
5	1226.25	Strong	C-O	Alcohol
6	1376.94	Medium	S-O	Sulfonyl Chloride
7	1662.59	Strong	C–C	Carboxylic Acid
8	1731.75	Medium	C–H	Aldehyde
9	2848.46	Medium	C–H	Alkenes
10	2915.92	Medium	C–H	Alkenes
11	3351.03	Medium	N–H	Amines

This observation is consistent with recent research, where XRD analysis confirmed the crystalline nature of AgNPs synthesized using various plant extracts. For instance, AgNPs synthesized using *Curcuma longa* flower extract exhibited a face centered cubic structure with an average particle size of approximately 5 nm.[27] Similarly, AgNPs synthesized using *Inula viscosa* extract displayed a face centered cubic crystal structure with a size of 15±5 nm. These studies underscore the influence of synthesis methods and plant extracts on the crystallinity and size of AgNPs.[28]

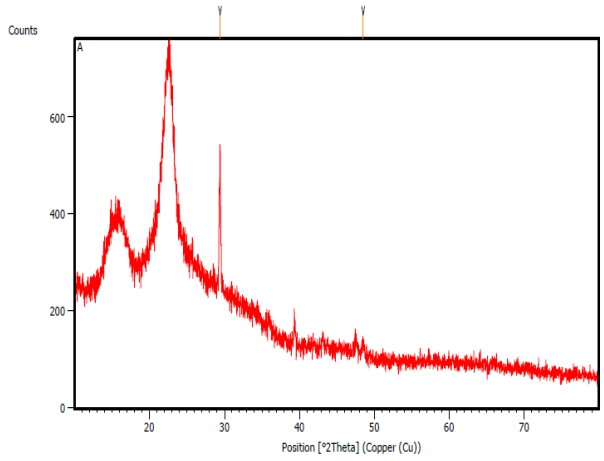

Figure 3: X-Ray Diffraction patterns analysis of synthesized silver nanoparticles

SEM Analysis

The SEM analysis offered visual confirmation of the form and size of the AgNPs (Fig. 4). The SEM images revealed predominantly spherical nanoparticles, a typical shape for AgNPs synthesized using plant extracts. SEM analysis confirmed the presence of AgNPs, supporting the successful synthesis of AgNPs. In a similar study involving *Quercus coccifera*, spherical AgNPs were also observed, composed of silver, carbon and oxygen.[29] Recent studies have further corroborated these findings. For instance, synthesized AgNPs using extracts from *A. wilhelmsii*, *M. chamomilla* and *C. longa*, observing spherical nanoparticles ranging from 10 to 20 nm in size. Their SEM analysis highlighted the uniformity and dispersion of the nanoparticles, emphasizing the role of phyto-chemicals in directing nanoparticle morphology.[25] Similarly, a previous study demonstrated that surface texture and uniformity observed through SEM play a crucial role in cytotoxicity. This underscores the importance of SEM in not only confirming nanoparticle synthesis but also in predicting their biological interactions.[30] Moreover, the study utilizing *Raphanus sativus, Ipomoea batatas and Ananas comosus* leaf extracts showcased SEM effectiveness in revealing agglomeration patterns, aiding in the assessment of particle stability in colloidal suspensions. Such morphological insights are vital for applications where nanoparticle stability is paramount.[31]

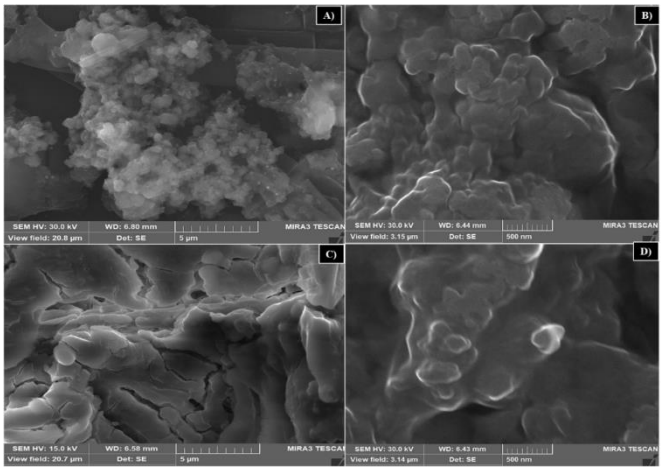

Figure 4: SEM analysis of the synthesized silver nanoparticles at different magnifications. **(A)** AgNPs imaged at approximately 4,160× magnification (scale bar: 5 µm, view field: 20.8 µm), showing clustered nanoparticle formation. **(B)** Higher magnification (~6,300×; scale bar: 500 nm, view field: 3.15 µm) revealing detailed surface morphology. **(C)** Aggregated AgNPs observed at ~4,140× magnification (scale bar: 5 µm, view field: 20.7 µm). **(D)** Close-up surface structure at ~6,280× magnification (scale bar: 500 nm, view field: 3.14 µm).

Dynamic Light Scattering (DLS) Analysis

The particle size distribution of the AgNPs generated using *T. terrestris* extract, as analyzed by DLS, is presented in (Fig. 5). From this figure, the particle size of 512.7 nm with a polydispersity index (PDI) of 0.340, indicating moderate uniformity. The intensity based size distribution revealed two peaks, with the dominant peak at 971.0 nm (80.1% intensity) and a smaller population at 199.6 nm (19.9% intensity), suggesting some degree of aggregation. Previous reports also showed similar nanoparticle size when synthesized by *Trigonella foenum graecum* L extract.[32]

Comparable findings were reported, the synthesized AgNPs using *Nigella sativa* seed extract and observed a bimodal distribution, with aggregation attributed to the presence of phenolic compounds and alkaloids acting as stabilizing agents.[33] Additionally, a previous study demonstrated that *Azadirachta indica* mediated AgNPs also displayed particle sizes above 500 nm under certain synthesis conditions, influenced by plant metabolite concentration and absence of post synthesis stabilization.[34] In contrast, a study using carrot extract demonstrated that the size distribution of synthesized AgNPs could be monodisperse or homogeneous when optimized with varying concentrations of $AgNO_3$ and adjusted pH values emphasizing the role of synthesis parameters in determining nanoparticle size and dispersion behavior.[35]

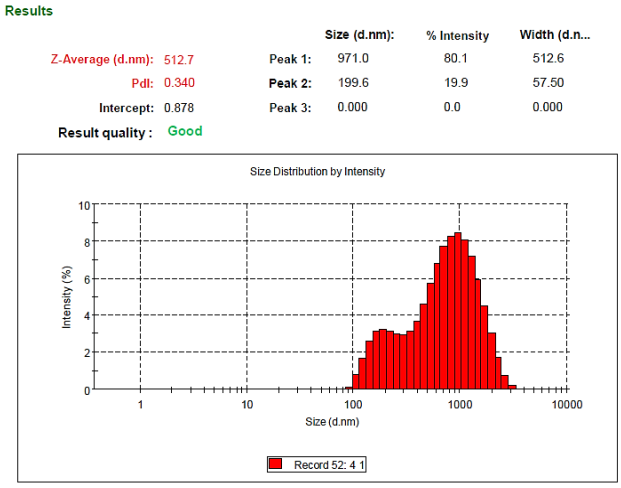

Figure 5: Particle size distribution of synthesized silver nanoparticles

In vitro Anti-oxidant Assays

DPPH Analysis

The anti-oxidant potential of AgNPs was assessed through the DPPH (2,2-diphenyl-1-picrylhydrazyl) assay, a commonly employed technique to measure free radical scavenging capacity. The results (Fig. 6a) showed significant scavenging activity, with the highest inhibition of 78.27% observed at a concentration of 640 µg/mL. This suggests that AgNPs effectively neutralize free radicals, indicating their potential as anti-oxidant. This ability to scavenge DPPH radicals is significant as it reflects the AgNPs capacity to reduce oxidative stress, which contributes to various diseases and aging. In a similar study, the free radicals formed by *Echinacea purpurea* had an IC_{50} range of 21.9 mg/mL to 39.6 mg/mL.[36]

In a similar study, AgNPs synthesized from *Ocimum sanctum* exhibited a maximum DPPH scavenging activity of 72.4% at 500 µg/mL, highlighting comparable efficacy in anti-oxidant potential.[37] Another study reported AgNPs synthesized using *Azadirachta indica*, showing an IC_{50} value of 28.6 µg/mL, further demonstrating strong radical scavenging activity.[38] These findings affirm that green synthesized AgNPs using plant extracts exhibit promising anti-oxidant properties, aligning with our current results. Additionally, in a separate study, the free radicals formed by *Echinacea purpurea* had an IC_{50} range of 21.9 mg/mL to 39.6 mg/mL, indicating lower anti-oxidant efficiency compared to silver nanoparticle formulations.[39]

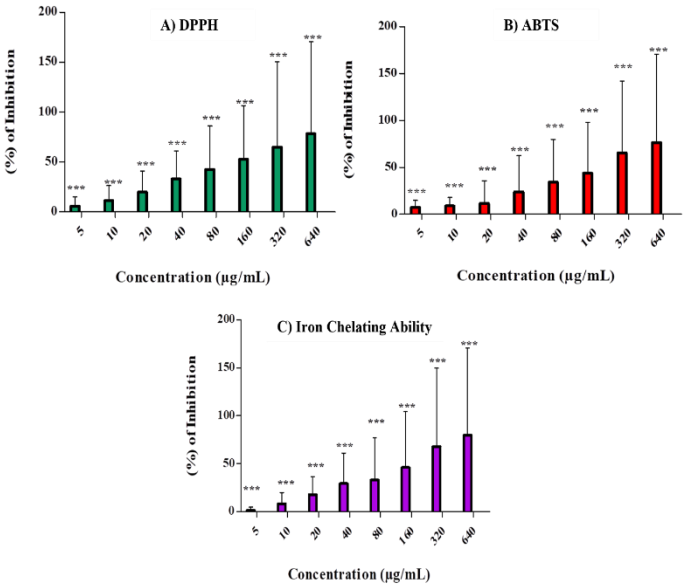

Figure 6: *In-vitro* antioxidant activities of synthesized silver nanoparticles were evaluated using a) DPPH, b) ABTS+ and c) Iron chelating ability assays. Results are expressed as Mean ± SD. Data analysis was conducted using one-way ANOVA, followed by Dunnett's multiple comparison tests to determine significant differences between treatments and the control group. Significance levels are indicated by asterisks (***P < 0.0001), denoting statistically significant differences compared to the control group.

ABTS Analysis

The ABTS assay was conducted to determine the AgNPs ability to neutralize ABTS radicals, another important method for evaluating anti-oxidant properties showed in Fig.6b. The AgNPs exhibited a maximum inhibition of 76.55% at a concentration of 640 µg/mL. This finding underscores the versatility of AgNPs in scavenging different types of free radicals, further supporting their potential as an alternative to traditional anti-oxidant. A similar study on nanoparticles from *Annona muricata* reported an IC_{50} value of 30.78 µg/mL.[40]

In recent years, several studies have highlighted the anti-oxidant properties of AgNPs synthesized from various plant sources. For instance, a study on AgNPs synthesized from guava leaf extract demonstrated a high ABTS radical scavenging activity of 85% at 640 µg/mL, aligning closely with the results of the present study. This highlights the significant anti-oxidant potential of AgNPs synthesized from plant materials.[41] Furthermore, AgNPs synthesized from *Fusarium oxysporum* have also shown superior anti-oxidant activity when compared to standard anti-oxidant like ascorbic acid and butylated hydroxytoluene, further reinforcing the potential of AgNPs as effective anti-oxidant.[42] In the case of *A. muricata*, a study on its aqueous leaf extracts revealed IC_{50} values of 50-100 µg/mL in the DPPH assay, indicating strong anti-oxidant activity. However, studies specifically focusing on AgNPs synthesized from *A. muricata* are limited. The present study IC_{50} value of 30.78 µg/mL for AgNPs derived from *A. muricata* suggests enhanced anti-oxidant properties compared to the leaf extract alone, likely due to the unique physico-chemical characteristics of nanoparticles, which facilitate better interaction with free radicals.[43]

Iron Chelating Ability
Iron chelation plays a vital role in anti-oxidant mechanisms by limiting the availability of free iron, which can catalyze reactive oxygen species (ROS) formation. The iron chelation capacity of AgNPs was evaluated (Fig. 6c), revealing a highest inhibition of 79.74% at 640 µg/mL, indicating significant binding to free iron ions. This ability contributes to AgNPs anti-oxidant activity and suggests that they may help mitigate oxidative damage by preventing iron induced ROS formation. A similar study on *Anoxybacillus flavithermus* AgNPs found an inhibition of 75.53% at 60 µg/mL.[44]

Another study of AgNPs have demonstrated significant anti-oxidant properties, partly due to their ability to chelate free iron ions, thereby limiting the formation of ROS. This mechanism is crucial in mitigating oxidative stress-related damages.[45] A study synthesized AgNPs using leaf extract of *Morus alba* and evaluated their anti-oxidant activities. The findings indicated that these nanoparticles exhibited effective metal ion chelating activity, contributing to their anti-oxidant potential.[46] In another research, AgNPs were synthesized using the rhizome extract of *Geum urbanum*. The study evaluated their anti-oxidant potential through various *in vitro* assays, including metal ion chelating activity, highlighting their role in scavenging free radicals and chelating metal ions.[47] These studies underscore the importance of iron chelation in the anti-oxidant mechanisms of silver AgNPs, suggesting their potential in mitigating oxidative stress and related pathologies.

Enzyme Assays
Peroxidase (POD) Assay
Peroxidase (POD) is involved in oxidative reactions, including the breakdown of hydrogen peroxide (H_2O_2) and organic peroxides. The AgNPs demonstrated significant inhibition of POD activity (Fig. 7a), with the highest inhibition of 91.99% at 640 µg/mL. This extraordinary result suggests that AgNPs may interfere with POD activity, potentially blocking it beyond its natural capacity. This effect could offer therapeutic applications in managing peroxidase related oxidative damage.[48]

Recent studies have explored the interaction between AgNPs and peroxidase activity in plants, revealing complex effects that vary with concentration and plant species. In a study on *Populus nigra* L. callus culture, exposure to biofunctionalized AgNPs-Cit-L-Cys led to a significant increase in ascorbate peroxidase (APX) and catalase (CAT) activities, particularly at lower concentrations (2.5 mg/L). This response was associated with oxidative stress indicators such as elevated lipid peroxidation levels, suggesting that AgNPs can induce oxidative stress, prompting an upregulation of anti-oxidant enzymes as a defence mechanism.[49]

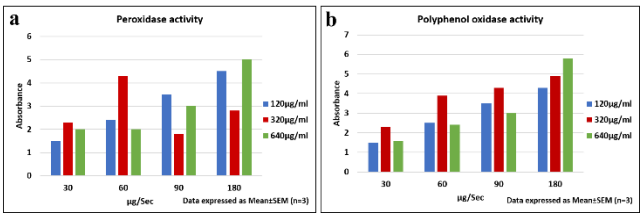

Figure 7: *In-vitro* Enzyme activity of Synthesized silver nanoparticles at different concentration a) Peroxidase Assay b) Polyphenol oxidase assay

Similarly, research on lettuce (*Lactuca sativa* L.) demonstrated that AgNPs application under varying irrigation regimes influenced physiological traits and enzyme activities. The study found that AgNPs could modulate anti-oxidant enzyme activities, including peroxidase, depending on the concentration and environmental conditions, indicating a potential role in enhancing plant stress tolerance.[50] These findings underscore the dual role of AgNPs in plant systems: at certain concentrations, they may induce oxidative stress, leading to an upregulation of anti-oxidant defences, while at higher concentrations, they can inhibit peroxidase activity, potentially overwhelming the plant's natural defence mechanisms. This duality highlights the importance of precise dosing and application strategies when considering AgNPs for agricultural or therapeutic purposes.[49]

Polyphenol Oxidase (PPO) Assay
PPO catalyzes the oxidation of phenolic compounds, which can lead to browning in plants and food products. The inhibition of PPO activity by AgNPs was evaluated (Fig. 7b). The AgNPs showed the highest inhibition of 98.74% at 640 µg/mL, suggesting that AgNPs can inhibit PPO, which could be beneficial in food preservation and in managing oxidative stress in biological systems.[51]

Recent studies have explored the application of AgNPs in modulating PPO activity within pharmaceutical and bio-medical contexts. For instance, research involving *Moringa oleifera* leaf extracts demonstrated that incorporating AgNPs enhanced the total anti-oxidant capacity and increased the concentration of polyphenolic compounds. This enhancement is attributed to the interaction between AgNPs and phenolic compounds, leading to improved scavenging activity against free radicals and increased cytotoxicity against colon cancer cells. Such findings suggest that AgNPs can play a significant role in managing oxidative stress in biological systems.[52]

Similarly, studies on *Calotropis procera* have investigated the synthesis and characterization of AgNPs using leaf extracts. These AgNPs exhibited notable anti-microbial properties, indicating their potential utility in pharmaceutical applications. While the primary focus was on anti-microbial activity, the interaction between AgNPs and plant extracts rich in phenolic compounds implies a possible influence on PPO activity, warranting further investigation.[53] These studies underscore the potential of AgNPs in inhibiting PPO activity, which could be beneficial in food preservation and in managing oxidative stress in biological systems.

In Vitro Anti-Proliferative Effect of Silver Nanoparticles on MG-63 Osteosarcoma Cell Line by MTT Assay
The anti-proliferative effects of AgNPs on the MG-63 osteosarcoma cell line were evaluated to explore their potential as anti-cancer agents. A dose dependent decrease in cell viability was observed, with a reduction to 78.34% at 80 µg/mL. The IC_{50} value, which represents the concentration at which 50% of cell proliferation was inhibited, was calculated to be 19.56 µg/mL (Fig. 8). These results indicate that AgNPs possess significant anti-cancer activity, effectively inhibiting the growth of osteosarcoma cells, which supports their potential in cancer therapy. Similar data from *Lagerstroemia speciosa* AgNPs also showed a decrease in cell viability, with an IC_{50} value of 37.57 µg/mL in the MG-63 cell line.[54]

Recent studies have highlighted the promising anti-cancer potential of AgNPs against osteosarcoma, particularly the MG-63 cell line. Our findings demonstrating a dose dependent cytotoxic effect with an IC_{50} of 19.56 µg/mL align with previous studies reporting that AgNPs not only inhibit MG-63 proliferation but also modulate the tumor immune microenvironment, enhancing therapeutic efficacy.[55]

Additionally, another study evaluated the impact of different AgNPs sizes and concentrations on MG-63 cells and confirmed their pro-apoptotic activity through ROS generation and mitochondrial dysfunction.[56] These findings underscore the significance of AgNPs in osteosarcoma treatment, highlighting their multifaceted roles in inducing apoptosis, modulating immune responses and suppressing proliferation. The consistent IC_{50} values and cellular responses across plant mediated AgNPs further reinforce their potential as novel, bio-compatible agents in osteosarcoma therapy.

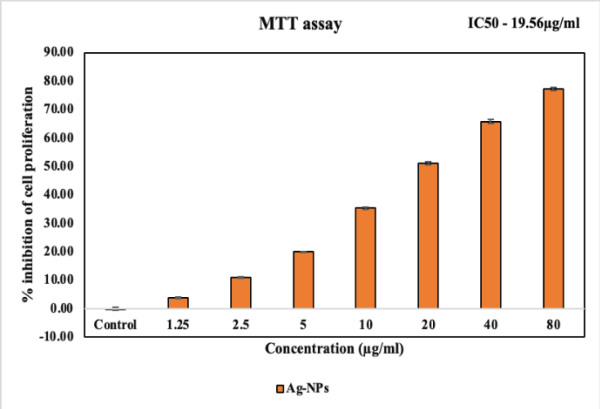

Figure 8: MTT assay confirming the anti-proliferative activity of silver nanoparticles against MG-63 Osteosarcoma Cell Line.

Gene Expression Studies

Gene expression analysis was conducted using quantitative real-time PCR (qRT-PCR) to explore the molecular mechanisms underlying the biological effects of AgNPs. The primary focus of this analysis was on the Bax, Caspase 9 and Bcl-2, following treatment with varying concentrations (10, 20 and 40 µg/ml) of AgNPs (Fig. 9). The results revealed a dose dependent upregulation of Bax and Caspase 9, with significant increases observed at higher concentrations, indicating activation of the intrinsic apoptotic pathway. In contrast, the anti-apoptotic gene Bcl-2 was significantly downregulated, supporting the pro apoptotic effect of AgNPs.

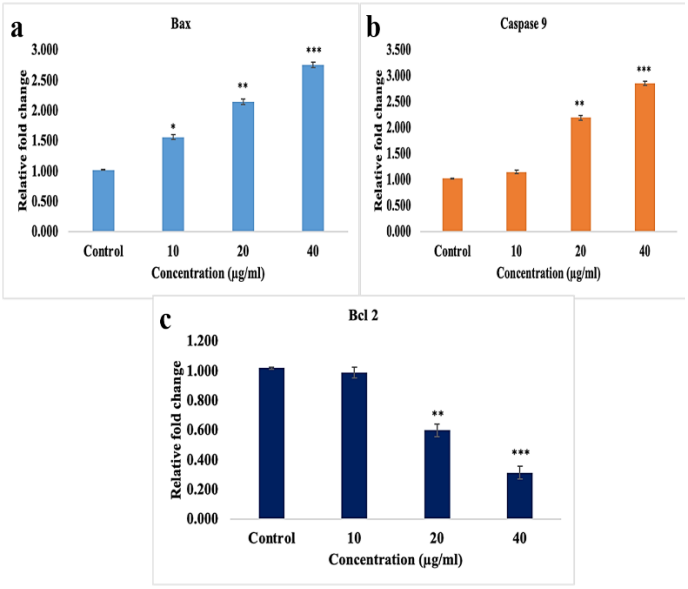

Figure 9: Gene Expression studies of synthesized silver nanoparticles at different assays a) Bax b) Caspase 9 c) Bcl-2

This gene expression profile suggests that AgNPs promote apoptosis through a mitochondrial mediated mechanism. In addition to their pro apoptotic effects in eukaryotic systems, AgNPs may also exert anti-bacterial actions through a different mechanism. Notably, AgNPs exposure has been linked to the downregulation of key bacterial porin genes, such as oprD and carO, which are crucial for maintaining cell membrane permeability and allowing the uptake of small molecules and nutrients. The suppression of these genes indicates that AgNPs might disrupt normal bacterial membrane function, impairing nutrient acquisition and enhancing susceptibility to anti-microbial agents. Together, these findings underscore the dual functional potential of AgNPs, acting both as pro apoptotic agents in mammalian systems and as anti-bacterial agents targeting microbial survival pathways.[57,58]

Conclusion

In conclusion, AgNPs synthesized from *T. terrestris* leaf extract show strong potential for therapeutic use, particularly in cancer treatment. The ecofriendly green synthesis method used here proves to be an efficient and cost-effective approach for nanoparticle production. Characterization of the AgNPs revealed key physico-chemical properties, including high surface area and stability, enhancing their biological activity. These nanoparticles demonstrated significant anti-oxidant effects, helping to counteract oxidative stress. Additionally, the AgNPs showed promising anti-cancer activity by inhibiting cell growth and inducing apoptosis in MG-63 osteosarcoma cells. Overall, *T. terrestris* derived AgNPs appear to be a promising option for cancer therapy, specifically in osteosarcoma. Further research is necessary to assess their *in vivo* effectiveness, molecular mechanisms and safety for clinical applications.

Conflict of Interest

The authors declare no conflict of interest.

Authors' Declaration

The authors hereby declare that the work presented in this article are original and that any liability for claims relating to the content of this article will be borne by them.

References

1. Saritha P, Arunprakash S, Srinivasan P, Al-Ansari MM, Singh S, Dixit S. Luminescent Silver Nanoparticles Biosynthesis Using *Couroupita guianensis* Flower Extract: Antibacterial and Anticancer Potential. Luminescence. 2024; 39(11): e70005.
2. Shahzadi S, Fatima S, Shafiq Z, Janjua MR. A review on green synthesis of silver nanoparticles (SNPs) using plant extracts: a multifaceted approach in photocatalysis, environmental remediation, and biomedicine. RSC Adv. 2025; 15(5): 3858-3903.
3. Mathanmohun M, Sagadevan S, Rahman MZ, Lett JA, Fatimah I, Moharana S, Garg S, Al-Anber MA. Unveiling sustainable, greener synthesis strategies and multifaceted applications of copper oxide nanoparticles. J Mol Struct. 2024; 1305: 137788.
4. Yadav S, Mali SN, Pandey A. Biogenic Nanoparticles as Safer Alternatives for Gastric Ulcers: An Update on Green Synthesis Methods, Toxicity, and Their Efficacy in Controlling Inflammation. Biol Trace Elem Res. 2024; 202 (11): 1-20.
5. Navaneethan RD, NCJ PL, Ramaiah M, Ravindran R, Chinnathambi A, Alharbi SA, Sivagnanam A, Mohemedibrahim PK. Caralluma pauciflora based Ag-NPs activate ROS-induced apoptosis through down-regulation of AKT, mTOR and pI3K signaling in human Gastric Cancer (AGS) cells. Nanotechnology. 2024; 35(19): 195102. https://doi.org/10.1088/1361-6528/ad26d9
6. Parvin SJ, Vijaya T. A review on *tribulus terrestris*: Insights into its medicinal properties and applications. Sustainable Innovations in Life Sciences: Integ Ecol Nanotechnol Toxicol. 2024, ISBN-13 (15): 1-7. https://doi.org/10.70593/978-81-982935-0-3_1

7. Osman AI, Zhang Y, Farghali M, Rashwan AK, Eltaweil AS, Abd El-Monaem EM, Mohamed IM, Badr MM, Ihara I, Rooney DW, Yap PS. Synthesis of green nanoparticles for energy, biomedical, environmental, agricultural, and food applications: A review. Environ Chem Lett. 2024; 22(2): 841-887.
8. Duman H, Eker F, Akdaşçi E, Witkowska AM, Bechelany M, Karav S. Silver nanoparticles: A comprehensive review of synthesis methods and chemical and physical properties. Nanomater. 2024; 14(18): 1527.
9. Darji SA, Tiwari P, Chandra A, Sharma A. Biological synthesis of nanoparticles from selected medicinal plants. Nanotechnol In Silico Tools, 2024: 47-59. https://doi.org/10.1016/B978-0-443-15457-7.00021-6
10. Benjamin MA, Mokhtar RA, Iqbal M, Abdullah A, Azizah R, Sulistyorini L, Mahfudh N, Zakaria ZA. Medicinal Plants of Southeast Asia with Anti-α-Glucosidase Activity as Potential Source for Type-2 Diabetes Mellitus Treatment. J Ethnopharmacol. 2024; 330: 118239.
11. Sivalingam AM, Pandian A. Identification and characterization of silver nanoparticles from *Erythrina indica* and its antioxidant and Uropathogenic antimicrobial properties. Microb Pathog. 2024; 190: 106635.
12. Gudkov SV, Burmistrov DE, Fomina PA, Validov SZ, Kozlov VA. Antibacterial Properties of Copper Oxide Nanoparticles. Int J Mol Sci. 2024; 25(21): 11563.
13. Giray G, Gonca S, Özdemir S, Isik Z, Yılmaz E, Soylak M, Dizge N. Novel extracellular synthesized silver nanoparticles using thermophilic *Anoxybacillus flavithermus* and Geobacillus stearothermophilus and their evaluation as nanodrugs. Prep Biochem Biotechnol. 2024; 54(3): 294-306.
14. Rana N, Banu AN, Kumar B, Singh SK, Abdel-Razik NE, Jalal NA, Bantun F, Vamanu E, Singh MP. Phytofabrication, characterization of silver nanoparticles using *Hippophae rhamnoides* berries extract and their biological activities. Front Microbiol. 2024;15:1399937.
15. Bras BS, do Nascimento Pereira I, Zibordi LC, Rosatto PA, Santos HH, Granero FO, Figueiredo CC, de Faria ML, Ximenes VF, de Moraes RO, Santiago PS. Green synthesis of silver nanoparticles using food supplement from *Avena sativa* L., and their antioxidant, antiglycation, and anti-aging activities: In vitro and in silico studies. Food Bioprod Process. 2024; 147: 175-188.
16. Meydan I, Seckin H, Kocak Y, Okumus E, Bekmezci M, Sen F. Evaluation of antioxidant, antibacterial and thermal stability properties of silver nanoparticles synthesised with *Infundibulicybe gibba* extract. Int J Environ Sci Technol. 2024; 21: 6957-6966.
17. Li R, He M, Cui Y, Ji X, Zhang L, Lan X, Wang L, Han Z, Xiao H. Silver-palladium bimetallic nanoparticles stabilized by elm pod polysaccharide with peroxidase-like properties for glutathione detection and photothermal anti-tumor ability. Int J Biol Macromol. 2024; 264: 130673.
18. Fang Y, Li Y, Zhong X, Peng J. Formulation and characterization of a novel anti-human bone cancer supplement from silver nanoparticles green-synthesized using *Allium sativum* l. Leaf aqueous extract. Inorg Chem Commun. 2024; 168: 112979.
19. Metwaly FE, Moghazy MA, Sheded MG, Mohamed AA. Green synthesis of silver nanoparticles using leaf extract of the hydrophyte *Persicaria senegalensis*: Preparation and antioxidant activity. Inorg Nano-Met Chem. 2024: 1-11. https://doi.org/10.1080/24701556.2024.2354504
20. Telange DR, Mahajan NM, Mandale T, More S, Warokar A. *Pongamia pinnata* seed extract-mediated green synthesis of silver nanoparticle loaded nanogel for estimation of their antipsoriatic properties. Bioprocess Biosyst Eng. 2024; 47(8): 1409-1431.
21. Bharathi VU, Thambidurai S. Green synthesized chitosan-coated iron oxide nanocomposite using *Cissus quadrangularis* plant extract for antibacterial, antioxidant and anticancer applications. Inorg Chim Acta. 2024; 572: 122293.
22. Rehman G, Umar M, Shah N, Hamayun M, Ali A, Khan W, Khan A, Ahmad S, Alrefaei AF, Almutairi MH, Moon YS. Green synthesis and characterization of silver nanoparticles using Azadirachta indica seeds extract: in vitro and in vivo evaluation of anti-diabetic activity. Pharmaceuticals. 2023; 16(12): 1677.
23. Palithya S, Gaddam SA, Kotakadi VS, Penchalaneni J, Challagundla VN. Biosynthesis of silver nanoparticles using leaf extract of *Decaschistia crotonifolia* and its antibacterial, antioxidant, and catalytic applications. Green Chem Lett Rev. 2021; 14(1): 137-152.
24. Hanisha R, Balaganapathy M, Eswar B, Kathirvelan P, Rajabathar JR, Siddiqui N, Dinakarkumar Y. Biogenic synthesis of silver nanoparticles using *Spirulina maxima* extract and their bactericidal activity. J Umm Al-Qura Uni Appl Sci. 2024. https://doi.org/10.1007/s43994-024-00203-4
25. Asefian S, Ghavam M. Green and environmentally friendly synthesis of silver nanoparticles with antibacterial properties from some medicinal plants. BMC Biotech. 2024; 24(1): 1-22. https://doi.org/10.1186/s12896-023-00828-z
26. Katta VK, Dubey RS. Green synthesis of silver nanoparticles using *Tagetes erecta* plant and investigation of their structural, optical, chemical and morphological properties. Mater Today: Proc. 2021; 45: 794-798.
27. Giri VA, Sastry SV, Kapoor A. Biomass-assisted green synthesis and characterization of silver nanoparticles using *Azadirachta indica*, *Ocimum basilicum*, and *Curcuma longa*: evaluation of antifungal potential. Biomass Convers Biorefi. 2023: 1-15. https://doi.org/10.1007/s13399-023-05177-7
28. Okka EZ, Tongur T, Aytas TT, Yılmaz M, Topel Ö, Sahin R. Green Synthesis and the formation kinetics of silver nanoparticles in aqueous *Inula viscosa* extract. Optik. 2023; 294: 171487. https://doi.org/10.1016/j.ijleo.2023.171487
29. Kocazorbaz EK, Moulahoum H, Tut E, Sarac A, Tok K, Yalcin HT, Zihnioglu F. Kermes oak (Quercus coccifera L.) extract for a biogenic and eco-benign synthesis of silver nanoparticles with efficient biological activities. Environ Technol Innov. 2021; 24: 102067.
30. Tripathi N, Goshisht MK. Recent advances and mechanistic insights into antibacterial activity, antibiofilm activity, and cytotoxicity of silver nanoparticles. ACS Appl Bio Mat. 2022; 5(4): 1391-1463.
31. Chandrasekaran M, Chinnaiyan U, Sivaprakasam S, Paramasivam S. Biogenic synthesis and characterization of silver nanoparticles using a combined leaf extract for anti-bacterial and biofilm inhibition properties. *Trop J Nat Prod Res*. 202; 9(3): 1089-1096.
32. Soheyli F, Hassani H, Darroudi M. Biosynthesis of selenium nanoparticles using *Trigonella foenum-graecum* L extract

and examination of their photocatalytic and cytotoxic properties. Int J Environ Sci Technol. 2025; 22(2): 1017-1028.

33. Vijayakumar S, Divya M, Vaseeharan B, Chen J, Biruntha M, Silva LP, Duran-Lara EF, Shreema K, Ranjan S, Dasgupta N. Biological compound capping of silver nanoparticle with the seed extracts of blackcumin (*Nigella sativa*): a potential antibacterial, antidiabetic, anti-inflammatory, and antioxidant. J Inorg Organomet Polym Mater. 2021; 31: 624-635.
34. Tahir H, Rashid F, Ali S, Summer M, Afzal M. Synthesis, characterization, phytochemistry, and therapeutic potential of *Azadirachta indica* conjugated silver nanoparticles: a comprehensive study on antidiabetic and antioxidant properties. Biol Trace Elem Res. 2024; 203: 2170-2185.
35. Pramasari N, Anjani AG, Muslikh FA, Lestari TP, Shoviantari F, Septyaningrum SD, Melati IS, Randy GY. Green synthesis, optimization and characterization of carrot extract silver nanoparticles. Trop J Nat Prod Res. 2024; 8(12): 9591-9595.
36. Gecer EN, Erenler R, Temiz C, Genc N, Yildiz I. Green synthesis of silver nanoparticles from *Echinacea purpurea* (L.) Moench with antioxidant profile. Part Sci Technol. 2022; 40(1): 50-57.
37. Ashokkumar M, Palanisamy K, Ganesh Kumar A, Muthusamy C, Senthil Kumar KJ. Green synthesis of silver and copper nanoparticles and their composites using *Ocimum sanctum* leaf extract displayed enhanced antibacterial, antioxidant and anticancer potentials. Artif Cells Nanomed Biotechnol. 2024; 52(1): 438-448.
38. Kumari SA, Patlolla AK, Madhusudhanachary P. Biosynthesis of silver nanoparticles using *Azadirachta indica* and their antioxidant and anticancer effects in cell lines. Micromachines. 2022; 13(9): 1416. https://doi.org/10.3390/mi13091416
39. Gecer EN, Erenler R, Temiz C, Genc N, Yildiz I. Green synthesis of silver nanoparticles from *Echinacea purpurea* (L.) Moench with antioxidant profile. Particul Sci Technol. 2022; 40(1): 50-57.
40. González-Pedroza MG, Argueta-Figueroa L, García-Contreras R, Jiménez-Martínez Y, Martínez-Martínez E, Navarro-Marchal SA, Marchal JA, Morales-Luckie RA, Boulaiz H. Silver nanoparticles from *Annona muricata* peel and leaf extracts as a potential potent, biocompatible and low cost antitumor tool. Nanomater. 2021; 11(5): 1273.
41. Jain A, Jangid T, Jangir RN, shankar Bhardwaj G. A Comprehensive Review on the Antioxidant Properties of Green Synthesized Nanoparticles: in vitro and in vivo Insights. Free Radic Antioxid. 2024; 14(2): 34-61.
42. El-Ansary AE, Omran AA, Mohamed HI, El-Mahdy OM. Green synthesized silver nanoparticles mediated by *Fusarium nygamai* isolate AJTYC1: characterizations, antioxidant, antimicrobial, anticancer, and photocatalytic activities and cytogenetic effects. Environ Sci Pollut Res. 2023; 30(45): 100477-100499.
43. Shaniba VS, Aziz AA, Joseph J, Jayasree PR, Manish Kumar PR. Synthesis, characterization and evaluation of antioxidant and cytotoxic potential of *Annona muricata* root extract-derived biogenic silver nanoparticles. J Clust Sci. 2022; 33: 467-483.
44. Giray G, Gonca S, Özdemir S, Isik Z, Yılmaz E, Soylak M, Dizge N. Novel extracellular synthesized silver nanoparticles using thermophilic *Anoxybacillus flavithermus* and *Geobacillus stearothermophilus* and their evaluation as nanodrugs. Prep Biochem Biotechnol. 2024; 54(3): 294-306.
45. Dara PK, Mahadevan R, Digita PA, Visnuvinayagam S, Kumar LR, Mathew S, Ravishankar CN, Anandan RJ. Synthesis and biochemical characterization of silver nanoparticles grafted chitosan (Chi-Ag-NPs): In vitro studies on antioxidant and antibacterial applications. SN Appl Sci. 2020; 2: 665. https://doi.org/10.1007/s42452-020-2261-y
46. Das D, Ghosh R, Mandal P. Biogenic synthesis of silver nanoparticles using S1 genotype of *Morus alba* leaf extract: characterization, antimicrobial and antioxidant potential assessment. SN Appl Sci. 2019; 1: 498. https://doi.org/10.1007/s42452-019-0527-z
47. Macovei I, Harabagiu V, Burlec AF, Mircea C, Horhogea CE, Rimbu CM, Săcărescu L, Panainte AD, Miron A, Hăncianu M, Nechita C. Biosynthesis of Silver and Gold Nanoparticles Using *Geum urbanum* L. Rhizome Extracts and Their Biological Efficiency. J Inorg Organomet Polym. Mater. 2024; 34(12): 5831-5853.
48. Kumari P, Azad C, Kumar RR, Kumari J, Aditya K, Kumar A. Defense inducer compounds up-regulated the peroxidase, polyphenol oxidase, and total phenol activities against spot blotch disease of wheat. Plant Pathol J. 2023; 39(2):159.
49. Iori V, Muzzini VG, Venditti I, Casentini B, Iannelli MA. Phytotoxic impact of bifunctionalized silver nanoparticles (AgNPs-Cit-L-Cys) and silver nitrate (AgNO3) on chronically exposed callus cultures of *Populus nigra* L. Environ Sci Pollut Res. 2023; 30(54): 116175-116185.
50. Kilic HK, Cakmakci T, Sensoy S. The application of nanoparticles on the physiological, morphological, enzyme activities, and nutrient uptake of lettuce under different irrigation regimes. Enviro Dev Sustain. 2025: 1-25. https://doi.org/10.1007/s10668-025-06120-8
51. Mawale KS, Praveen A, Giridhar P. Efficacy of copper and silver nanoparticles on seedling growth, biochemical and antioxidant potential of *Capsicum annuum* L., in vitro and ex vitro. S Afr J Bot. 2024; 175: 1-14.
52. Shousha WG, Aboulthana WM, Salama AH, Saleh MH, Essawy EA. Evaluation of the biological activity of *Moringa oleifera* leaves extract after incorporating silver nanoparticles, in vitro study. Bull Nat Res Cent. 2019; 43(1): 212-225.
53. Nagime PV, Shaikh NM, Shaikh SB, Lokhande CD, Patil VV, Shafi S, Syukri DM, Chidrawar VR, Kumar A, Singh S. Facile synthesis of silver nanoparticles using *Calotropis procera* leaves: unraveling biological and electrochemical potentials. Discover Nano. 2024; 19(1): 139. https://doi.org/10.1186/s11671-024-04090-w
54. Khandare K, Kumar S, Sharma SC, Goswami S. Green synthesis of silver nanoparticles from supercritical CO2 mediated *Lagerstroemia speciosa* extract: Characterization, antimicrobial and antibiofilm activity. Biochem Biophys Res Commun. 2024; 739: 150967.
55. Hao P, Yang L, Yan Y, Wang X, Yin J, Hong W, Wang S, Yin X, Liu S. Metal-based nanocomposites for immunotherapy of osteosarcoma. Adv Compos Hybrid Mater. 2024; 7(6): 200. https://doi.org/10.1007/s42114-024-01030-1
56. Shi P, Cheng Z, Zhao K, Chen Y, Zhang A, Gan W, Zhang Y. Active targeting schemes for nano-drug delivery systems

in osteosarcoma therapeutics. J Nanobiotechnol. 2023; 21(1): 103-130.
57. Tripathi S, Mahra S, Sharma S, Mathew S, Sharma S. Interaction of Silver Nanoparticles with Plants: A Focus on the Phytotoxicity, Underlying Mechanism, and Alleviation Strategies. Plant Nano Biol. 2024; 9: 100082.
58. Katarzyńska-Banasik D, Kowalik K, Sechman A. Influence of silver nanoparticles on mRNA expression of thyroid hormone-related genes in the thyroid gland and liver of laying hens. Domest Anim Endocrinol. 2024; 86: 106820.